Science of the Total Environment 674 (2019) 264–278

Contents lists available at ScienceDirect

Science of the Total Environment

journal homepage: www.elsevier.com/locate/scitotenv

Patterns of outdoor exposure to heat in three South Asian cities

Cor Jacobs [a,*], Tanya Singh [a], Ganesh Gorti [b], Usman Iftikhar [c], Salar Saeed [d], Abu Syed [e,f], Farhat Abbas [c], Bashir Ahmad [g], Suruchi Bhadwal [b], Christian Siderius [a,h]

[a] Wageningen University and Research, Wageningen Environmental Research, Wageningen, the Netherlands
[b] The Energy and Resources Institute, Earth Science and Climate Change Division, New Delhi, India
[c] Government College University, Faculty of Engineering, Faisalabad, Pakistan
[d] Pakistan Agricultural Research Council, Islamabad, Pakistan
[e] Bangladesh Centre for Advanced Studies, Dhaka, Bangladesh
[f] Nansen-Bangladesh International Centre for Coastal, Ocean and Climate Studies, Dhaka, Bangladesh
[g] National Agricultural Research Center, Climate, Energy and Water Resources Institute, Islamabad, Pakistan
[h] London School of Economics and Political Science, Grantham Research Institute, London, United Kingdom

HIGHLIGHTS

- Exposure to heat is examined in Delhi, Dhaka, and Faisalabad.
- Extremely hot conditions were found to persist for prolonged periods of time.
- Spatial patterns of exposure are distinctly different between day and night.
- Informal neighbourhoods are diverse, but tend to remain warmer during the night.
- Heat action plans should be based on thermal indices.

GRAPHICAL ABSTRACT

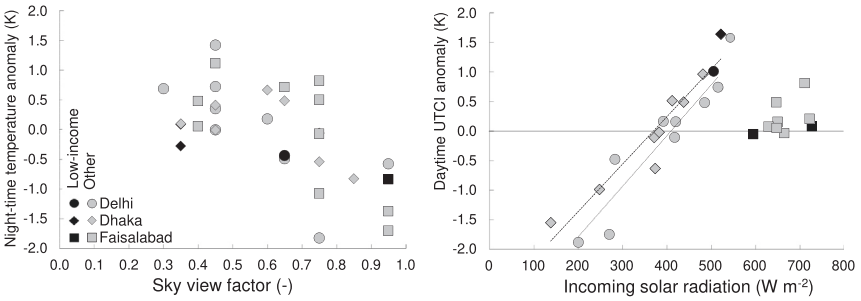

ARTICLE INFO

Article history:
Received 21 December 2018
Received in revised form 6 April 2019
Accepted 6 April 2019
Available online 9 April 2019

Editor: SCOTT SHERIDAN

Keywords:
Heat exposure
HI
WBGT
UTCI
Urban heat island
South Asia

ABSTRACT

Low socio-economic status has been widely recognized as a significant factor in enhancing a person's vulnerability to climate change including vulnerability to changes in temperature. Yet, little is known about exposure to heat within cities in developing countries, and even less about exposure within informal neighbourhoods in those countries. This paper presents an assessment of exposure to outdoor heat in the South Asian cities Delhi, Dhaka, and Faisalabad. The temporal evolution of exposure to heat is evaluated, as well as intra-urban differences, using meteorological measurements from mobile and stationary devices (April–September 2016). Exposure to heat is compared between low-income and other neighbourhoods in these cities. Results are expressed in terms of air temperature and in terms of the thermal indices Heat Index (HI), Wet Bulb Globe Temperature (WBGT) and Universal Thermal Climate Index (UTCI) at walking level. Conditions classified as dangerous to very dangerous, and likely to impede productivity, are observed almost every day of the measurement period during daytime, even when air temperature drops after the onset of the monsoon. It is recommended to cast heat warnings in terms of thermal indices instead of just temperature. Our results nuance the idea that people living in informal neighbourhoods are consistently more exposed to heat than people living in more prosperous neighbourhoods. During night-time, exposure does tend to be enhanced in densely-built informal neighbourhoods, but not if the low-income neighbourhoods are more open, or if they are embedded in green/blue areas.

* Corresponding author at: Wageningen Environmental Research, PO Box 47, 6700 AA Wageningen, the Netherlands.
E-mail address: cor.jacobs@wur.nl (C. Jacobs).

https://doi.org/10.1016/j.scitotenv.2019.04.087

1. Introduction

Climate change is expected to exacerbate the frequency, intensity, and duration of heatwaves (Collins et al., 2013). Exposure to extreme heat can lead to increased mortality and morbidity (Hajat et al., 2010a), even in regions where people are used to being exposed to hot conditions and therefore are expected to be adapted (Azhar et al., 2014; Singh et al., 2018). It has been postulated that there is a physical adaptability limit to heat, which may be reached in some regions of the world, depending on the temperature increases because of climate change (Sherwood and Huber, 2010). An analysis of documented extreme heat events with increased mortality showed that large parts of the world already experience lethal heat conditions and that climate change will lead to many more lethal heat events, notably in tropical and sub-tropical regions (Mora et al., 2017).

Low socio-economic status has been widely recognized as a factor that enhances a person's vulnerability to climate change including vulnerability to increasing temperature (Leichenko and Silva, 2014). In developing countries, a significant fraction of people with low socio-economic status inhabit so-called informal urban areas or slums. Despite attempts to avoid their formation or growth, the existence of such neighbourhoods is linked to rapid urbanization in many parts of the world (Ooi and Phua, 2007). These neighbourhoods are characterized by overcrowding, poor housing, high building fraction that may hamper natural ventilation by wind, meagre hygienic and sanitation conditions, and lack of infrastructure, including limited access to health care systems (Revi et al., 2014; Sverdlik, 2011). According to a recent study, they are also found at locations with comparatively rapid changes of temperature variability (Bathiany et al., 2018). This enhances the vulnerability of their inhabitants.

It is well-known that urban areas are warmer than rural areas on average. This phenomenon is known as the urban heat island (UHI) effect and is often particularly pronounced during the night (Oke, 1982). Urban characteristics at neighbourhood scale such as vegetation cover and building density and height, which are closely related to sky view, are important determinants of the average UHI strength (Stewart and Oke, 2012). High building density and lack of vegetation in informal or slum areas may imply enhanced exposure to heat, in particular during the night. Unfortunately, research on heat patterns within cities in low- to middle-income countries with dense urban areas is comparatively rare (Hondula et al., 2017) and little is known about heat exposure in such neighbourhoods.

Whereas some papers characterize the UHI of (South-) Asian cities (Santamouris, 2015; Tzavali et al., 2015; Kotharkar et al., 2018), many of those investigations are based on observations of surface temperature instead of ambient air temperature (e.g., Shastri et al., 2017) and reports of traverse measurements are comparatively rare (Kotharkar et al., 2018). Such studies on heat exposure were often carried out in isolation and mostly apply to limited periods of time, typically one to a couple of days, although two seasons were covered in the study by Yadav and Sharma (2018). At the time of writing we are unaware of studies specifically focusing on informal neighbourhoods or slum areas in South Asia.

Whether people feel comfortable with the microclimate they are exposed to, depends on a complex interaction between physical, physiological, behavioural, and psychological factors (Nikolopoulou and Steemers, 2003). Many thermal indices are available to describe the link between environmental conditions and thermal perception or comfort (Blazejczyk et al., 2012; de Freitas and Grigorieva, 2017). Environmental conditions affecting thermal comfort include air temperature, humidity, wind speed and radiation (shortwave and longwave). For example, trees as well as buildings provide shading, leading to improved thermal comfort in hot conditions, despite minimal differences in air temperature (Armson et al., 2012; Klemm et al., 2015). These environmental parameters, and therewith thermal comfort, are all strongly modified in the urban environment (van Hove et al., 2015). Unfortunately, South Asian studies on outdoor thermal comfort are quite rare (Kotharkar et al., 2018).

The main aim of the present paper is to assess possibly enhanced exposure to outdoor heat in informal urban neighbourhoods. We will characterize intra-urban differences in exposure to heat in three major cities in the South Asian region: Delhi (India), Dhaka (Bangladesh) and Faisalabad (Pakistan). This region is considered to be a climate change hotspot, defined as an area "where a strong climate change signal is combined with a large concentration of vulnerable, poor, or marginalized people" (De Souza et al., 2015).

The analysis presented in this paper utilizes traverse observations carried out weekly to bi-weekly, using the same type of instrumentation and the same measurement protocol in all three cities. We consider the day-time as well as the night-time situation throughout these months covering the pre-monsoon until the post-monsoon period and combine results from the traverse measurements with measurements at fixed stations. Furthermore, we assess exposure to heat in outdoor microclimatic conditions in terms of thermal indices instead of just UHI or air temperature. Because of these characteristics, our observations allow a rather unique direct comparison between three different cities and analysis of spatiotemporal patterns of outdoor exposure to heat, during a considerable part of the year.

2. Methods

2.1. General

Our assessment builds upon three sets of complementary observations. Traverse observations of air temperature and humidity, wind speed and solar radiation were performed using a collection of instruments placed on top of a car (Sections 2.3 and 2.4). The traverse measurements were complemented with observations at automatic weather stations (AWS) placed in the urban environment (Section 2.5). These measurements were used to determine temporal patterns and to correct the traverse observations for temporal trends. Finally, we collected data from official stations reporting to the World Meteorological Organization (WMO) in these three cities. The combination of micrometeorological measurements applied here allows evaluating spatial patterns of the most frequently used thermal indices (Section 2.6).

2.2. Study areas

The observations were carried out in Delhi (India), Dhaka (Bangladesh) and Faisalabad (Pakistan), three large cities in the Indo-Gangetic plain, one of the most densely populated areas in the world. Strong growth in population is expected, estimated at 40% (Delhi), 56% (Dhaka) and 52% (Faisalabad) until the year 2030 (compared to 2015), with strong urbanization (United Nations, 2014). Much of this growth in urban population will be accommodated, at least initially, through informal or low-income neighbourhoods which can be found in all three cities.

Delhi is India's capital and biggest city with nearly 25 million inhabitants (United Nations, 2014). Urban parts of Delhi cover about 700 km^2, out of nearly 1500 km^2 for the total Delhi area (India Census, 2015). Its climate can be classified as an overlap between humid subtropical and semi-arid and is highly influenced by the monsoon in July–September. The summer months are hot and increasingly humid towards the onset of the monsoon. In the hottest months, April–June, daily maximum temperatures can rise to between 40 °C and 45 °C, with minima remaining over 25 °C (Sati and Mohan, 2017). While daytime maxima decrease somewhat during the monsoon period, night-time minima on average remain over 25 °C until August, with average morning relative humidity being over 60% (Weatherbase, 2018a).

Dhaka is the capital of Bangladesh. It covers about 306 km^2 (Bangladesh Bureau of Statistics, 2014) and hosts about 19 million

inhabitants (United Nations, 2014). Dhaka's climate can be classified as a tropical savanna climate, with a distinct monsoonal season. The highest daily maximum temperatures are reached in March–May, the average being about 33 °C. However, maxima may rise to nearly 40 °C on individual days. Furthermore, the highest average minimum temperature of over 26 °C is observed in the monsoon months June–August. These months are also extremely humid, with an average evening relative humidity of about 75% and an average morning relative humidity of about 93% (Weatherbase, 2018b).

Faisalabad is home to about 3.2 million people and is the third largest city of Pakistan (Pakistan Bureau of Statistics, 2018). The surface area of the municipality of Faisalabad is about 210 km^2 (Minallah et al., 2012). Faisalabad has a dry, semi-arid climate, classified as mid-latitude steppe and desert climate and characterized by high temperature variability (Weatherbase, 2018c) and an increasing number of hot days, warm nights and heatwaves (Abbas, 2013; Saeed et al., 2016). The hottest months are May–July with maxima sometimes going up to around 50 °C in June and minima remaining around 27 °C from June–August, but sometimes exceeding 30 °C (Abbas, 2013).

2.3. Traverse measurements

Traverse measurements were performed to determine intra-urban spatial differences in air temperature, humidity, solar radiation, wind speed, and derived heat indices. Temperature was measured using a 0.25 mm fast response thermocouple (5TC-TT-TI-30-1M, Omega, USA; g in Fig. 1) and a HMP60 temperature and humidity probe (Vaisala, Finland; h). From the latter device we also obtained the humidity. Wind speed was measured using a 2-D ultrasonic anemometer (Windsonic, Gill Instruments, UK; f) and solar radiation with an upward facing pyranometer (SP-110, Apogee Instruments, USA; d).

The instruments were attached to a small polycarbonate cabinet (CAB PC 302018G, Fibox, the Netherlands), which housed the data logger (CR850, Campbell Scientific, UK; b), a flash memory drive (SC115, Campbell Scientific, UK; b) and a battery (YPC2A12, Yuasa, USA; b). Furthermore, the box was equipped with a GPS device for position logging (GPS 16X-HVS, Garmin, USA; c). The fast response temperature sensor was mounted inside a ventilated plastic tube to prevent radiation errors. A fan (D341T-012GK-2, Micronel, Switzerland; a) ensured an air flow through the tube at a speed of 4.6 ms^{-1}. The inlet of the tube was wrapped in aluminium tape and located above the front windscreen. The box was attached on top of a car using a set of four strong magnets (E834, Eclipse Magnetics, UK), see Fig. 1. The height of the measurements was about 2 m, depending a bit on the height of the car used.

Accuracy of the fast response thermocouple was between 0.5 and 1.0 °C, its time constant was 0.5 s. Radiation accuracy was ±5%, wind speed accuracy was ±2% at 12 ms^{-1}, temperature accuracy of the temperature-humidity probe was 0.6 °C and relative humidity (RH) accuracy was ±3% (0–90% RH) or ±5% (90–100% RH). GPS position accuracy was <15 m.

The typical driving speed with the instrumented cars was 5–10 ms^{-1} (18–36 kmh^{-1}), depending on traffic. Data were logged at a 2-second interval. This implies a spatial resolution of our measurements of 10–20 m. Measured wind speed was corrected for driving speed (using the GPS data) with a routine made available by Smith and Bourassa (1996).

The traverse measurements were carried out weekly from April to June and biweekly from July to September, in 2016, along fixed, predetermined transects (see Section 2.4). On a measurement day two runs were generally performed, one daytime and one night-time run. The daytime observations were carried out just after noon, around the time when the maximum temperature is usually reached, with the sun near its maximum elevation and solar radiation potentially highest. It was decided to start the night-time run shortly after sunset, encompassing the part of the day when the UHI often is most intense according to UHI development theory (Oke, 1982) as well as observations in Asian cities (Santamouris, 2015; Tzavali et al., 2015). Changes in background meteorological conditions due to diurnal variations are also expected to be relatively small during the periods chosen here, which avoids the need of large temporal trend corrections. In total 96 runs could be completed, of which 94 could be further analysed, 35 in Delhi, 35 in Dhaka and 24 in Faisalabad.

One run typically took 1.5–2 h, depending on traffic. Temporal trends can occur during such a period which may hide or exaggerate spatial differences between neighbourhoods. Therefore, using data from the AWS (see below), simple linear detrending was applied to the spatial temperature data (cf. Heusinkveld et al., 2014). As expected, night-time trends were usually negative while daytime trends were found to be negative or positive, which may be expected because observations were carried out around the time when maximum temperature was reached, so in practice sometimes before and sometimes after the temperature peak. Absolute values of computed trends usually remained well below 1 K per hour, but during 9 runs larger trends were found, up to a maximum of 1.45 K per hour.

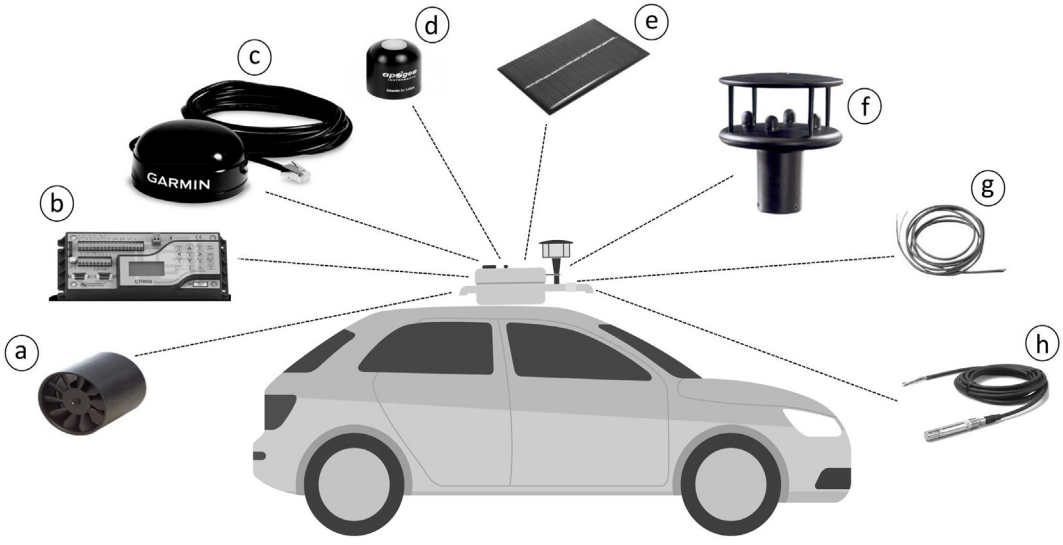

Fig. 1. Exploded view diagram of the device for traverse measurements: a) fan for ventilation; b) data logger with flash drive and battery; c) GPS device; d) solar radiation sensor; e) solar panel in support of energy supply; f) 2D sonic anemometer; g) fast response thermocouple; h) temperature and humidity probe.

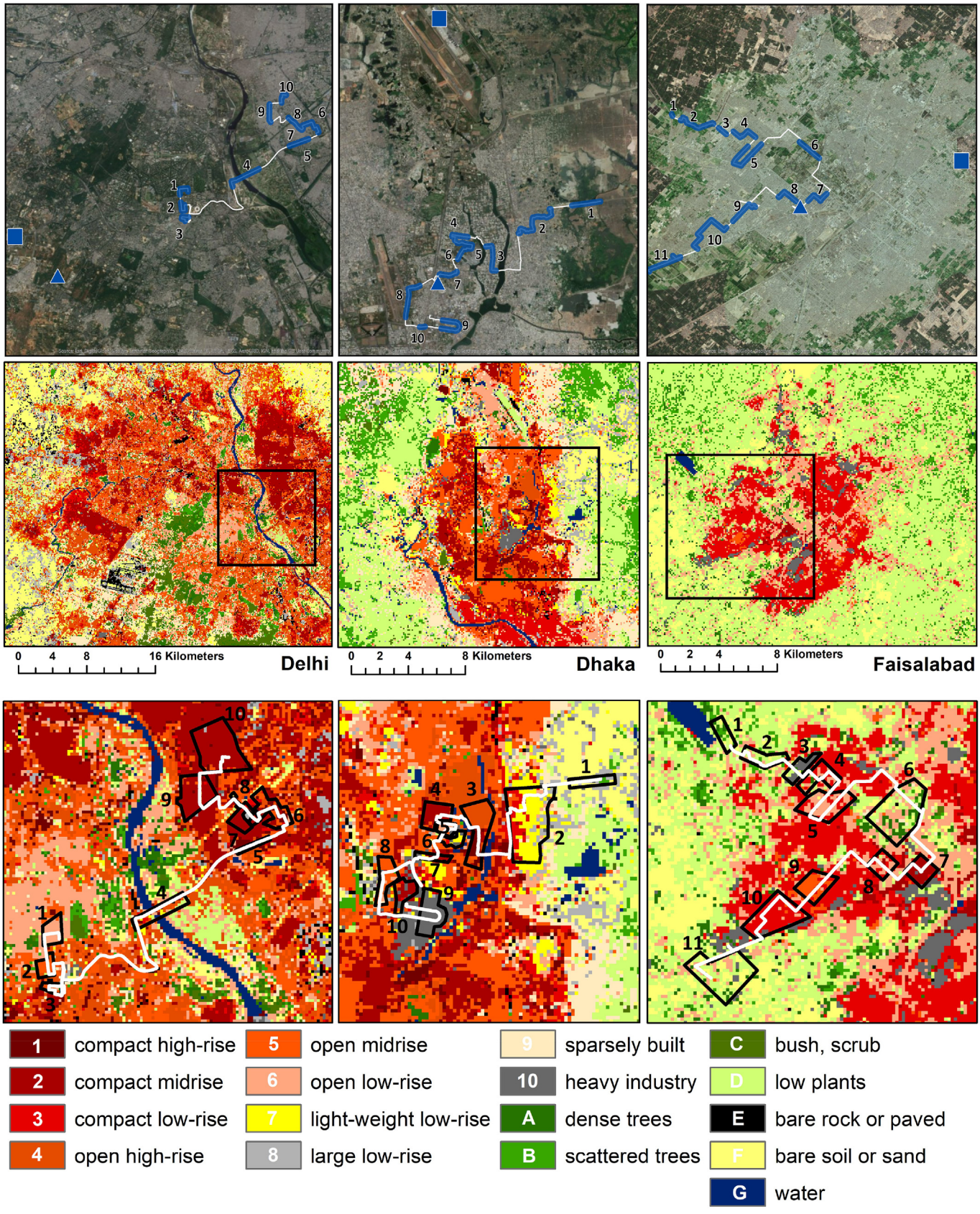

Fig. 2. Upper panel: Google Earth® maps showing the transects (white lines) and sections through selected neighbourhoods (in blue) for averaging the transect data for Delhi (left), Dhaka (middle) and Faisalabad (right). Middle panels: LCZ classification (Stewart and Oke, 2012) of the cities and the region. Lower panels: LCZ classification within the black squares shown in the middle panel with transects (white lines) and neighbourhood definition (black polygons). The blue triangles and squares in the upper panels indicate the locations of the AWS and WMO stations, respectively. The numbers correspond to the transects in Table 1.

2.4. Transects

In each city, fixed transect routes were selected to allow sampling of various differing target neighbourhood types, including informal neighbourhoods with a high density of buildings and little green as well as neighbourhoods with low building density and large green cover or water elements. The neighbourhoods were selected by visual inspection of Google Earth® images in combination with local knowledge. Average values of air and thermal comfort indices (see Section 2.6) were determined for the transect parts running through each target neighbourhood (Fig. 2).

The cities were also mapped in terms of so-called Local Climate Zones (LCZs) (Stewart and Oke, 2012). LCZs accommodate a clustering of urban characteristics (related to, for example, building density, height of roughness elements and urban metabolism) representing approximate ability to influence the local microclimate. They provide an objective classification for the purpose of studying physical aspects of urban climate studies. For further interpretation of the differences between neighbourhoods the dominant LCZ was determined in each of the target neighbourhoods, as indicated in Table 1. To classify the neighbourhoods in terms of LCZ the methodology proposed by Bechtel et al. (2015) was used. Briefly, Google Earth® images are used to designate training areas, which are areas with a known LCZ classification. The training areas are then linked to remotely sensed surface characteristics, notably Landsat satellite data, and subsequently extrapolated to the area of interest using the data from the training area. The results can then be verified against local knowledge and, if necessary, be adjusted by including new training data. The procedure can be repeated several times until the result matches the situation. A comparison of the abundance of the various LCZ in the three cities can be found in Table SI.I1. The resolution of the LCZ map is 100 m × 100 m.

Finally, the socio-economic status of the neighbourhoods was assessed, based on local knowledge. A distinction was made between high-income, middle-income, and low-income neighbourhoods. Sometimes, an intermediate classification was chosen. Some neighbourhoods are barely populated and were therefore classified in terms of their main land use (rural, green, road, industrial).

2.5. Stationary measurements

An AWS was installed in each of the three cities to determine the temporal evolution of the weather in the cities. The station (Wireless Vantage Pro2 Plus, Davis Instruments, USA) included solar radiation sensors and a daytime fan-aspirated radiation shield for the temperature and humidity devices. Furthermore, wind speed and wind direction were measured using a cup anemometer and wind vane, respectively. The station was also equipped with a rain gauge and a barometer. All sensors were measured at an interval of 1 min and the readings were subsequently averaged or summed to obtain hourly values. These hourly values were stored and uploaded to a server. Accuracies were: wind speed 0.5 ms^{-1}, air temperature 0.5 °C, relative humidity 2%, pressure 1 hPa, rainfall 4% for rates up to 100 $mm\ hr^{-1}$, solar radiation 5%.

Data from the AWS were used to determine temporal trends of weather variables during a transect run and to correct the spatial observations for this temporal trend. Therefore, locations of AWS were selected to represent an urban setting. Practical considerations such as the risk of vandalism further determined the selection of the location. The locations are indicated in Fig. 2. Daily results like maxima and averages were used if at least two-thirds of the hourly values were available for a specific day.

Although we focus on thermal comfort instead of on UHI, we also assessed UHI strength for completeness. Given the urban location of the AWS, their data could not be used to determine the UHI as defined by Oke (1982). Therefore, our UHI assessments were based on data from nearby weather stations in Delhi, Dhaka, and Faisalabad, run by the national weather services and which should conform to guidelines

Table 1
Naming and classification of neighbourhoods sampled by the transect parts indicated in Fig. 2. Coding combines socio-economic classification with dominant LCZ classification (see Fig. 1). For Delhi, this leads to two cases in which the coding would be the same (Low/Middle-2). Hence, we added "a" and "b" to distinguish between these neighbourhoods. "Fraction" is the percentage of neighbourhood grid points (100x100m) in the dominant LCZ. For each LCZ the typical sky view range is given (Stewart and Oke, 2012).

City	Transect #	Socio-economic	Neighbourhood code		Dominant LCZ	Fraction (%)	Sky view
Delhi	1	High.Income	High-6	HI-6	6	88	0.6–0.9
	2	Middle.Income	Middle-5	MI-5	5	74	0.5–0.8
	3	Low/Middle.Income	Low/Middle-5	LMI-5	5	52	0.5–0.8
	4	Green/Road	Green/Road-4	GR-4	4,D	32	0.5–0.7
	5	Low.Income	Low-2	LO-2	2	47	0.3–0.6
	6	Middle.Income	Middle-1	MI-1	1	37	0.2–0.4
	7	Low/Middle.Income	Low/Middle-2a	LMI-2	2	87	0.3–0.6
	8	Green	Green-D	GR-D	D	50	0.9–1.0
	9	Middle.Income	Middle-2	MI-2	2	88	0.3–0.6
	10	Low/Middle.Income	Low/Middle-2b	LMI-2b	2	92	0.3–0.6
Dhaka	1	Rural	Rural-8	RU-8	8	45	0.7–1.0
	2	Low/Middle.Income	Low/Middle-7	LMI-7	7	50	0.2–0.5
	3	High.Income	High-4	HI-4	4	63	0.5–0.7
	4	High.Income	High-2	HI-2	2	84	0.3–0.6
	5	Low/Middle.Income	Low/Middle-6	LMI-6	6	63	0.6–0.9
	6	Low.Income	Low-7	LO-7	7	37	0.2–0.5
	7	Middle.Income	Middle-2	MI-2	2	42	0.3–0.6
	8	Middle.Income	Middle-5	MI-5	5	72	0.5–0.8
	9	Middle.Income	Middle-10	MI-10	10	92	0.6–0.9
	10	Low/Middle.Income	Low/Middle-2	LMI-2	2	52	0.3–0.6
Faisalabad	1	Rural	Rural-D	RU-D	D	32	0.9–1.0
	2	Low.Income	Low-D	LO-D	D	48	0.9–1.0
	3	Industry	Industry-10	IN-10	10	69	0.6–0.9
	4	Middle.Income	Middle-3	MI-3	3	60	0.2–0.6
	5	High/Middle.Income	High/Middle-6	HMI-6	6	60	0.6–0.9
	6	Green	Green-6	GR-6	6	33	0.6–0.9
	7	Low/Middle.Income	Low/Middle-2	LMI-2	2	91	0.3–0.6
	8	High.Income	High-6	HI-6	6	44	0.6–0.9
	9	Middle.Income	Middle-5	MI-5	5	65	0.5–0.8
	10	Low.Income	Low-3	LO-3	3	88	0.2–0.6
	11	Rural	Rural-D	RU-D	D	46	0.9–1.0

issued by the World Meteorological Organization (WMO). Henceforth, these stations will be called "WMO stations." Mean UHI intensity was determined by subtracting the temperatures observed at the WMO stations from the average detrended transect temperature in the corresponding time slots. The maximum UHI strength observed along the transects was also computed, using the neighbourhood mean temperatures.

2.6. Thermal indices

Apart from air temperature as influenced by the UHI we consider three thermal indices to acknowledge that human thermal comfort and heat stress depend on other weather variables too. Like explained below, the indices differ in their response to weather variables. The first index is the Heat Index (HI [°C]), a well-known index belonging to the category of indices allowing assessment of the thermal environment from standard weather variables. HI has been widely used in, for example, the United States to forecast and communicate heat conditions to the general public. An apparent temperature is constructed using a fit of the actual air temperature and the relative humidity on Steadman's (Steadman, 1979a; Steadman, 1979b) apparent temperature (Blazejczyk et al., 2012):

$$\mathrm{HI} = -8.784695 + 1.61139411 \cdot T + 2.338549 \cdot RH - 0.14611605 \cdot T \cdot RH - 1.2308094 \cdot T^2 - 1.6424828 \cdot 10^{-2} \cdot RH^2 + 2.211732 \cdot 10^{-3} \cdot T^2 \cdot RH + 7.2546 \cdot 10^{-4} \cdot T \cdot RH^2 - 3.582 \cdot T^2 \cdot RH^2 \quad (1)$$

where T [°C] is the air temperature and RH [%] is the relative humidity. Although the data underlying the fit include effects of wind speed and radiation, HI will only respond to temperature and humidity. For communication purposes such a simpler approach may be an advantage.

The second index we will use is the Wet Bulb Globe Temperature (WBGT) (Budd, 2015):

$$\mathrm{WBGT} = 0.7T_{wn} + 0.2T_G + 0.1\,T \quad (2)$$

where T_{wn} is the naturally ventilated wet bulb temperature, and T_G is the so-called globe temperature. The WBGT has a strong history in industrial health protection. It responds to radiation exchange by means of the temperature of the black globe, designed to mimic human radiation exchange with the environment. Normally, T_G is measured inside a sealed, thin-walled black globe with a diameter of 15 cm. However, here we follow Liljegren et al. (2008), who proposed a model that appears to be able to reliably estimate WBGT using measured incoming solar radiation, air temperature, wind speed and humidity, with a good estimate of T_G as an intermediate product.

We then use the computed T_G to estimate the mean radiant temperature, T_{mrt} [°C] (Thorsson et al., 2007), which in turn is used to compute our third index, the Universal Thermal Climate Index (UTCI [°C]). This index is based on a dynamic model describing thermoregulation of the human body, considering the governing principles of the human body's energy balance. To that end, it considers the relevant meteorological parameters as well as thermo-physiological and clothing parameters (Fiala et al., 2012; Havenith et al., 2012; Jendritzky et al., 2012). To compute UTCI we used the polynomial fit made available at www.utci.org (Brode et al., 2012), which requires T, T_{mrt}, RH (or vapour pressure) and wind speed (u [ms^{-1}]) as input:

$$\mathrm{UTCI} = \mathrm{f}(T, T_{mrt}, u, RH) \quad (3)$$

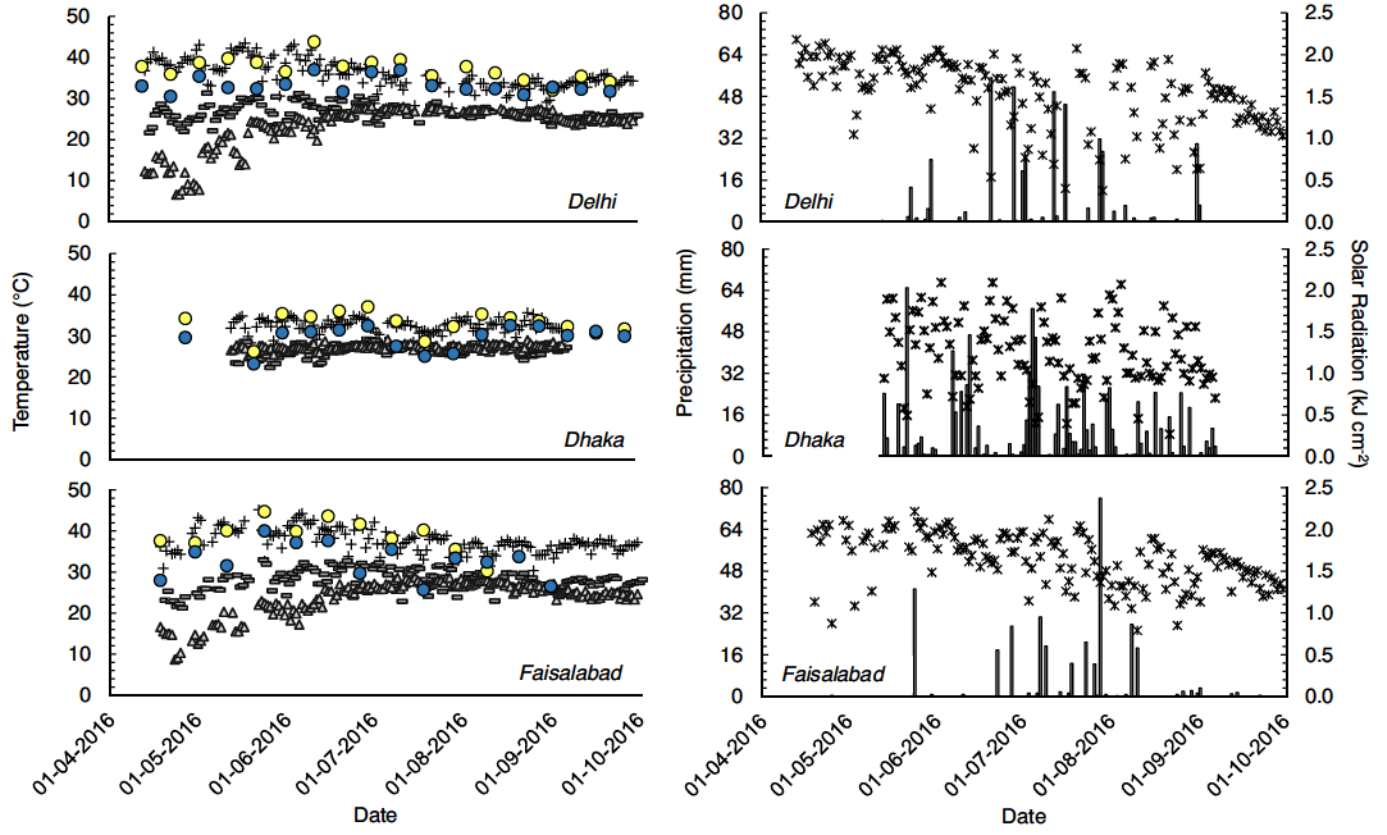

Fig. 3. Weather conditions in Delhi (upper), Dhaka (middle) and Faisalabad (lower) in the summer of 2016. The left panels show maximum temperature (pluses), minimum temperature (dashes) and maximum dew point temperature (triangles). Also shown are the average temperatures of the transects during daytime (light yellow circles) and in the early evening (dark blue circles). The right panels show daily sums of precipitation (columns, left axis) and incoming solar radiation (stars, right axis).

UTCI then refers to "the air temperature of the reference condition causing the same model response as the actual condition", with the reference condition defined as a person with a walking speed of 4kmh ^{1} and a metabolic heat production of 135Wm ^{2} in an environment where u at a height of 10 m is 0.5 ms ^{1}, $T_{mrt} = T$ and $RH = 50\%$ up to a vapour pressure of 20 hPa. Used in this way, UTCI allows objective quantification and comparison of the thermal environment people are exposed to; it is not intended to evaluate thermal perception, heat stress or heat strain of specific individuals at a specific location. Wind speed u from our measurements was recomputed to a value representing the wind speed at a height of 10 m, according to the guidelines for UTCI computation (Brode et al., 2012). The method assumes a logarithmic wind profile, which probably does not occur within cities (Oke et al., 2017). Nevertheless, the assumption is not a critical one if the main goal is standardisation for the purpose of comparison of spatiotemporal patterns. Given the uncertainty regarding urban wind profiles, we decided to adopt the standard approach. If u after extrapolation to a height of 10 m was out of the validity range for the fit (3), that is, <0.5 ms ^{1}, we computed UTCI using $u = 0.5$ ms ^{1}.

2.7. Evaluation of spatial differences

After the measurements of a run were completed, all data were downloaded from the data logger and processed with the statistical software R (R Core Team, 2013). Averages of all variables, x, were computed per neighbourhood transect, being the part of the city transect

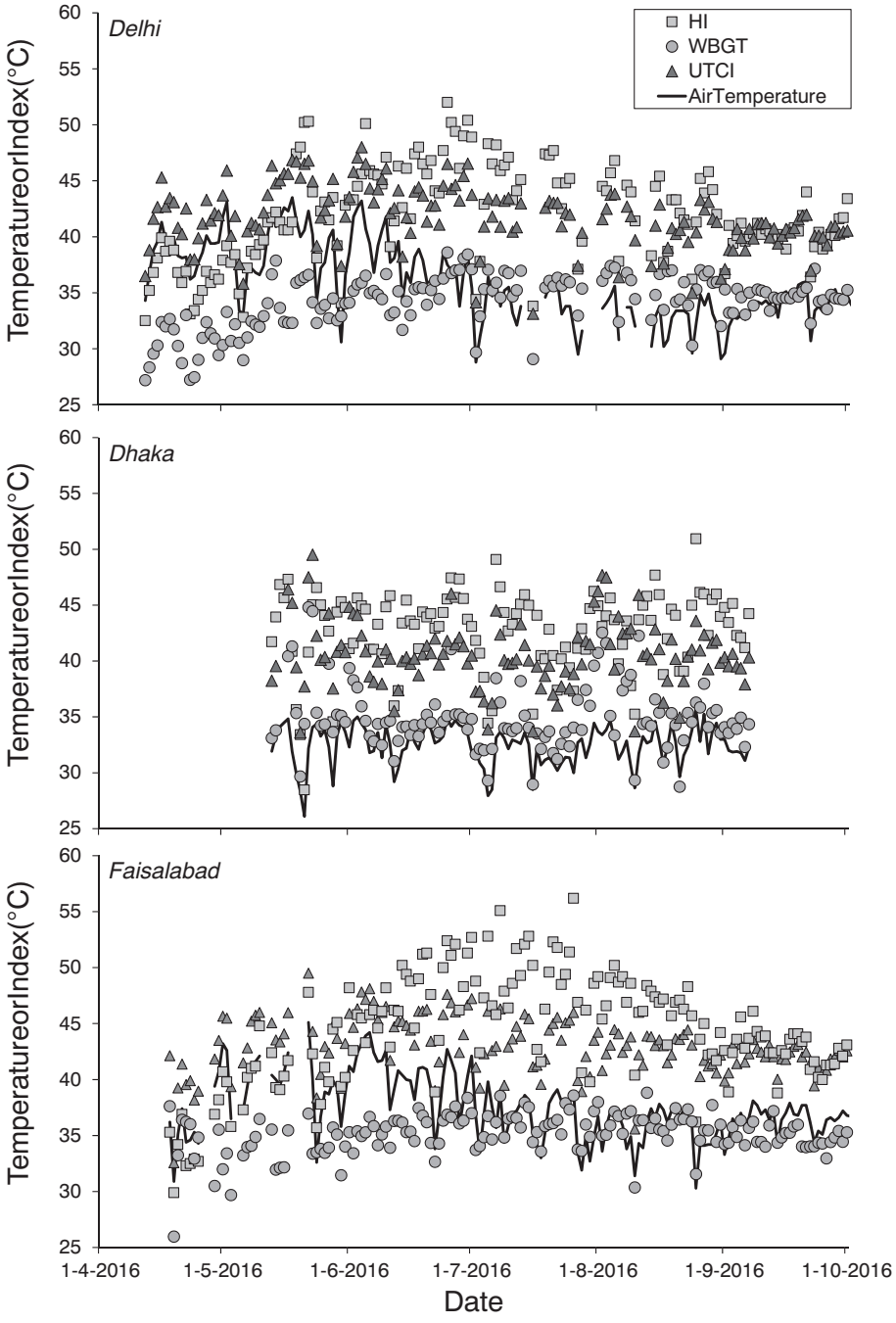

Fig. 4. Seasonal course of daily maximum air temperature, HI, WGBT and UTCI for Delhi (upper), Dhaka (middle) and Faisalabad (lower).

running through predefined polygons (see Section 2.4 and Fig. 2). These polygons delineated distinct neighbourhoods that were based on Google Earth® satellite images, from which physical neighbourhood characteristics were estimated (building density, amount of green), combined with local knowledge on socio-economic status and were fine-tuned based on local inspection before the start of the measurement campaigns.

Here, spatial anomalies determined per run are used to examine spatial differences. For variable x the spatial anomalies are defined as the difference between the overall mean for all neighbourhoods considered and its mean for a specific neighbourhood:

$$x'_n = x_n \quad \overline{x} \tag{4}$$

Here x_n denotes the mean of the variable considered (temperature or one of the heat indices) for a specific neighbourhood n (1–10 in Delhi or Dhaka and 1–11 in Faisalabad), $\overline{x}$ denotes the average over all transect parts considered and x'_n symbolizes the anomaly computed for neighbourhood n. Since the anomalies are determined per run, all runtime spatial averages of x'_n are zero by definition.

Between-neighbourhood means were compared using a robust variant of the one-way ANOVA test by applying the Welch's t-test adjustment, after hypothesis testing of equal variances across groups was conducted (Field et al., 2012). As a post hoc test for the pairwise comparisons between each neighbourhood the Bonferroni correction was applied.

3. Results

3.1. Weather conditions

Fig. 3 provides a general impression of the weather conditions during the summer period of 2016 in the three cities, using our measurements at the AWS. The time series confirm the expectations from the climatic situations in the city.

In Delhi, maximum temperature rose to over 40 °C on some days in the hottest period and minimum temperatures generally varied between 25 °C and 30 °C. Notably in April and May, the maximum dew point temperature was far below the air temperatures, showing that the humidity was quite low. In this period, the weather was generally fair, with daily solar radiation totals between 1.5 and 2.0kJcm ^{2} and hardly any precipitation. Upon the onset of the monsoon the air temperatures dropped somewhat, but the humidity rose dramatically, with maximum dew point temperatures approximately equal to the minimum temperature. Precipitation occurred regularly and the variation in incoming solar radiation illustrates the difference in cloudiness among the days in that period.

The course of weather conditions in Faisalabad is similar to that in Delhi, although the radiation intensity is much less variable so that its gradual seasonal decrease becomes clearly visible. By contrast, Dhaka shows limited variation in heat and moisture conditions. Maximum temperature varies between 30 °C and 35 °C, minimum temperature is around 25 °C. The humidity is high during the entire period, with maximum dew point temperatures approaching the minimum temperatures. This is also caused by the frequent precipitation, which often falls in large amounts. The daily radiation load is quite variable throughout the season, which is indicative of variable cloud cover.

More details on the weather conditions on the days of traverse measurements are provided in the Supplementary information (SI.II). Here, we depict in Fig. 3 the average air temperature along the transects after detrending. The daytime temperatures from the transects approximately follow the maximum temperature of the AWS. Like expected, the evening transect temperatures are usually well above the minimum temperature, and below the maximum temperature.

Table 2
Heat stress classification based on daily maxima of thermal indices from observations with AWS. Threshold values are taken from Blazejczyk et al. (2012) for HI and WBGT, and from www.utci.org for UTCI.

Index and threshold	Classification/city	From days with reliable maxima		
		Delhi	Dhaka	Faisalabad
Total number	–	190	115	186
HI > 54 °C	Sweltering (extreme danger)	0	0	2
HI = 41 to 54 °C	Very hot (danger)	92	89	125
WBGT>30 °C	Sweltering (extreme danger)	166	110	175
WBGT = 28 to 30 °C	Very hot (danger)	18	5	8
UTCI>46 °C	Extreme heat stress	11	7	18
UTCI = 38 to 46 °C	Strong heat stress	139	87	146

3.2. Seasonal trend of the heat indices

The seasonal development of the heat indices in the three cities studied is shown in Fig. 4. The figure depicts the daily maximum value of indices along with the maximum air temperature, using hourly averages from the AWS.

HI, WBGT and UTCI only follow T to a limited extent, in Delhi and Faisalabad in particular. In these cities, maximum T varies strongly around 40 °C in the hottest, pre-monsoon period and then declines somewhat to values around 32–35 °C in June–July. However, HI and WBGT continue to increase and UTCI hardly changes in those months. This behaviour can be explained by the strong increase in atmospheric humidity (see Fig. 3). Only as of August the indices follow T again and trends become similar. In Dhaka, there is hardly any trend in any of the indices during the period shown here. Comparatively large day-to-day variations in WBGT and UTCI can be explained by the large variability in solar radiation (see Fig. 3). A notable feature is that in periods when T in Dhaka is clearly lower than in the other cities, between 30 and 35 °C versus around 40 to 45 °C in Delhi and Faisalabad, the values of WBGT and UTCI in Dhaka are still at levels similar to the ones in Delhi and Faisalabad, around 35 °C for WBGT and 45° for UTCI. Also, HI is only slightly lower in Dhaka, around 45 °C versus 45°–50° in the other cities. Only HI in Faisalabad in July stands out with values up to 55 °C.

In terms of heat stress risk, focussing on the daily maxima of the indices, potentially dangerous levels of thermal stress could occur on most days of the observational period, and in all three cities (Table 2). To evaluate heat stress conditions, we use the set of threshold values quoted in Blazejczyk et al. (2012) for HI and WBGT and the UTCI assessment scale available from www.utci.org. It appears that in Dhaka the WBGT surpasses the 28 °C threshold ("very hot to sweltering") each day for which observations are available (n = 115), of which on 110 days

Table 3
UHI intensities [K] during periods of transect measurements. Reference temperature used here was obtained from weather stations run by national meteorological services ("WMO stations"). "Mean UHI" refers to temperature differences averaged over the analysed parts of all transects (see Section 2.4). "Max UHI" refers to temperature differences between the WMO station and the warmest part of a transect. Average, max and min denote the seasonal averages, maxima, and minima, respectively. 'n' denotes the number of measurement days included.

Quantity	Delhi		Dhaka		Faisalabad	
	Day (n = 17)	Night (n = 13)	Day (n = 17)	Night (n = 18)	Day (n = 11)	Night (n = 13)
Average mean UHI	1.0	3.4	0.6	0.7	0.0	1.4
Max mean UHI	3.2	5.7	1.7	2.8	1.1	3.2
Min mean UHI	1.3	1.5	0.2	0.3	0.6	0.3
Average max UHI	2.5	4.9	1.6	1.5	0.8	3.0
Max max UHI	5.0	8.0	3.2	3.5	2.2	5.9
Min max UHI	0.1	2.8	0.3	0.1	0.2	0.9

(95%) the >30 °C level is reached ("sweltering"). Working in such conditions would become too dangerous for normally trained people. Similarly, the 28 °C level for WBGT is reached on 184 out of 190 days (97%) in Delhi and on 183 out of 186 days in Faisalabad. According to UTCI very strong to extreme heat stress (UTCI >38 °C) could occur on 79% of the observation days in Delhi, on 82% in Dhaka and on 88% in Faisalabad, with extreme heat stress conditions (UTCI >46 °C) occurring on 6% of the days in Delhi and Dhaka and on nearly 10% of the days in Faisalabad. The maximum in the radiation driven indices will be reached in sunny conditions. HI is basically insensitive to such conditions and indicates somewhat less severe heat stress conditions: HI exceeds the 41 °C threshold ("very hot to sweltering") on 48% of the days in Delhi, 76% in Dhaka and 68% in Faisalabad.

3.3. Spatial differences

For completeness, we first describe some observed characteristics of the UHI. Estimated mean, minimum, and maximum UHI intensities are shown in Table 3 for daytime UHI and night-time (evening) UHI. The daytime UHI intensity is generally weaker than the night-time one, like expected from theory (Oke, 1982). The results for Delhi confirm estimates by Mohan et al. (2012, 2013) and Yadav and Sharma (2018).

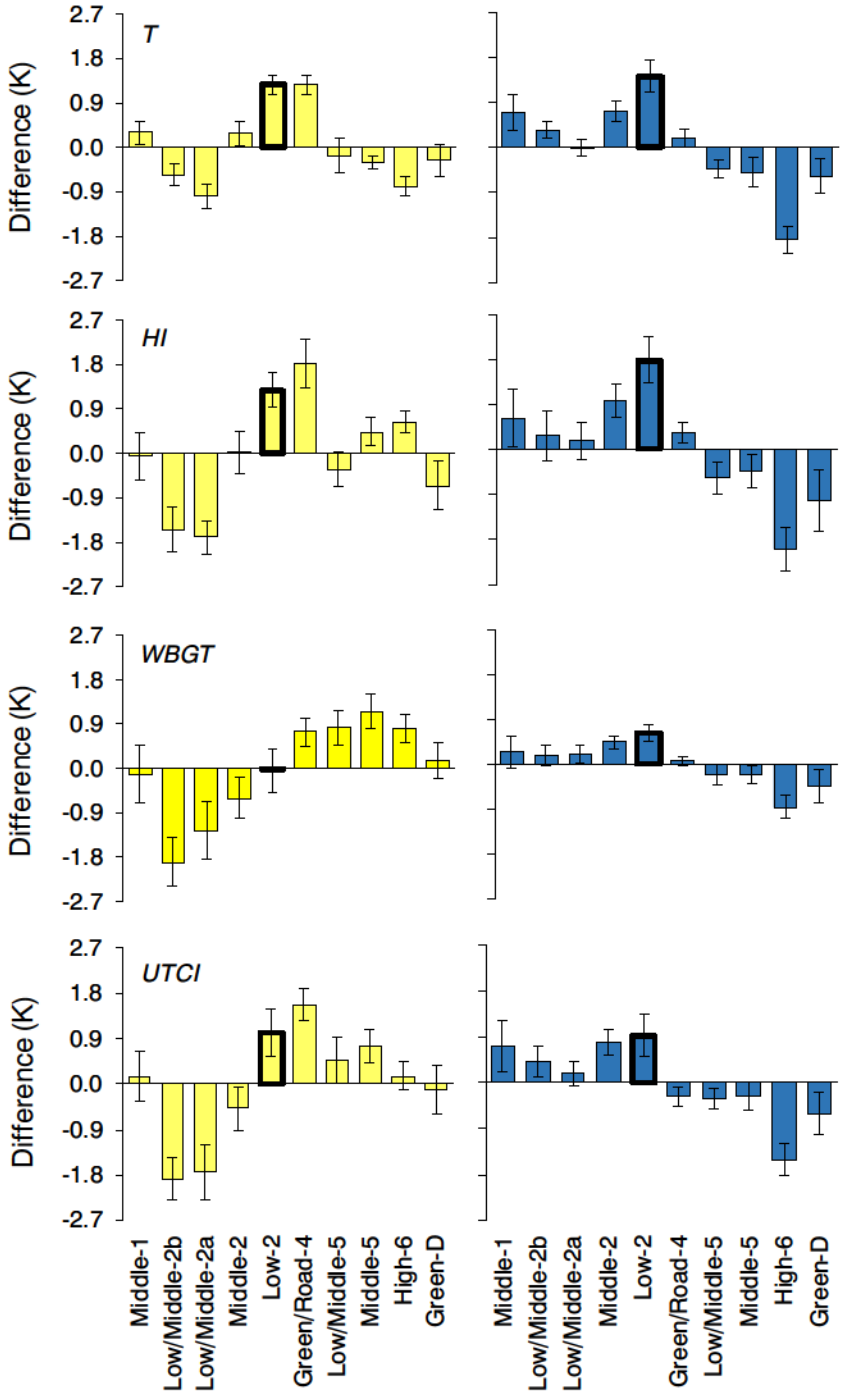

Fig. 5. Average anomaly of (from top to bottom) T, HI, WBGT and UTCI for the neighbourhoods studied in Delhi. Data are ordered from the left to the right according to increasing sky view factor of the main LCZ, using the middle values for the LCZ. See Table 1 for neighbourhood characteristics, LCZ and sky view values. Low-income neighbourhoods have been highlighted (bars with thick black border). Left: daytime; right: night-time. The error bars indicate the 95% confidence interval.

Daytime and night-time UHI intensity and the differences between them are quite small in Dhaka, which may be due to the frequent precipitation with associated cloudiness. It is well-known that UHI development is stronger on clear and calm days (Oke, 1982; Theeuwes et al., 2017). The largest UHI effect is obtained in some transect parts of Delhi, where UHI strengths up to 8 K were observed. In Faisalabad UHI intensities up to nearly 6 K were obtained.

Figs. 5–7 show the seasonal mean of x'_n from all traverse measurements in Delhi, Dhaka, and Faisalabad, respectively, for all variables considered here. The data have been ordered from left to right according to increasing sky view factor, so that densely built neighbourhoods are found at the left of the graphs and more open ones to the right. The error bars show the 95% confidence interval of the seasonal averages per neighbourhood and indicate that most of the differences are statistically significant (see SI.III results for the ANOVA test and pairwise *t*-tests for the individual transects, confirming true differences between neighbourhood mean temperatures in the vast majority of cases). In Delhi, average seasonal anomalies of air temperature vary between −1.0 and +1.3 K for daytime conditions. Average night-time anomalies vary between −1.4 and +1.8 K. So, average intra-urban temperature differences were 2.3 K during the afternoon transects and 3.2 K during the evening transect. In Dhaka, the intra-urban differences were smaller, amounting to 1.4 and 1.5 K for midday and evening conditions, respectively. Faisalabad also shows somewhat smaller daytime

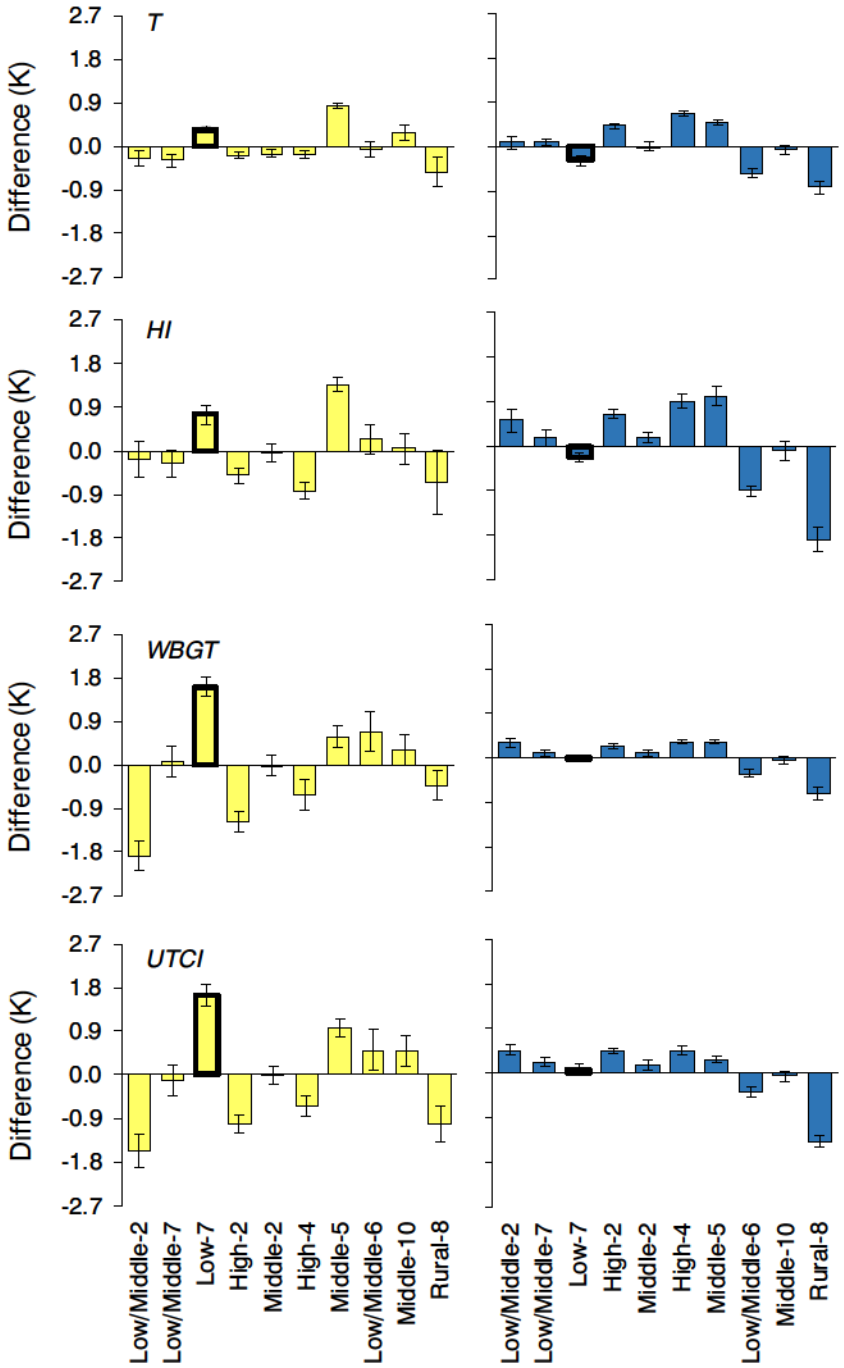

Fig. 6. As in Fig. 5, but for Dhaka.

differences, 1.4 K, but larger differences during the evening, 2.8 K. These results are in line with the general behaviour of the UHI, which is usually larger during the night (Oke, 1982; also see Table 1).

Especially during the night, the more densely built neighbourhoods (LCZ 1–3, 7), among which the informal neighbourhoods classified as LCZ 7, tend to be among the warmer ones. Greener and more open neighbourhoods tend to be cooler, like expected from the LCZ classification (Stewart and Oke, 2012), but the differences are not entirely consistent. In Dhaka some inconsistencies seem to occur, but here, the differences are small anyway, since cloudy weather conditions often preclude development of strong intra-urban differences. In Faisalabad some of the more open neighbourhood (Middle-5 and High-6) appear to be comparatively warm. During the afternoon some of the densely built transects may be among the cooler ones, for example, "Low/Middle-2a" and "Low/Middle-2b" in Delhi, "High-2" in Dhaka and "Middle-3" in Faisalabad, although the differences in the latter city are generally very small during daytime. In Dhaka, the industrial area is among the hotter ones during daytime, possibly because of the anthropogenic heat production.

The relationship between sky view and night-time temperature is further investigated in Fig. 8. Low-income neighbourhoods are highlighted (bold symbols). The figure broadly confirms the expected

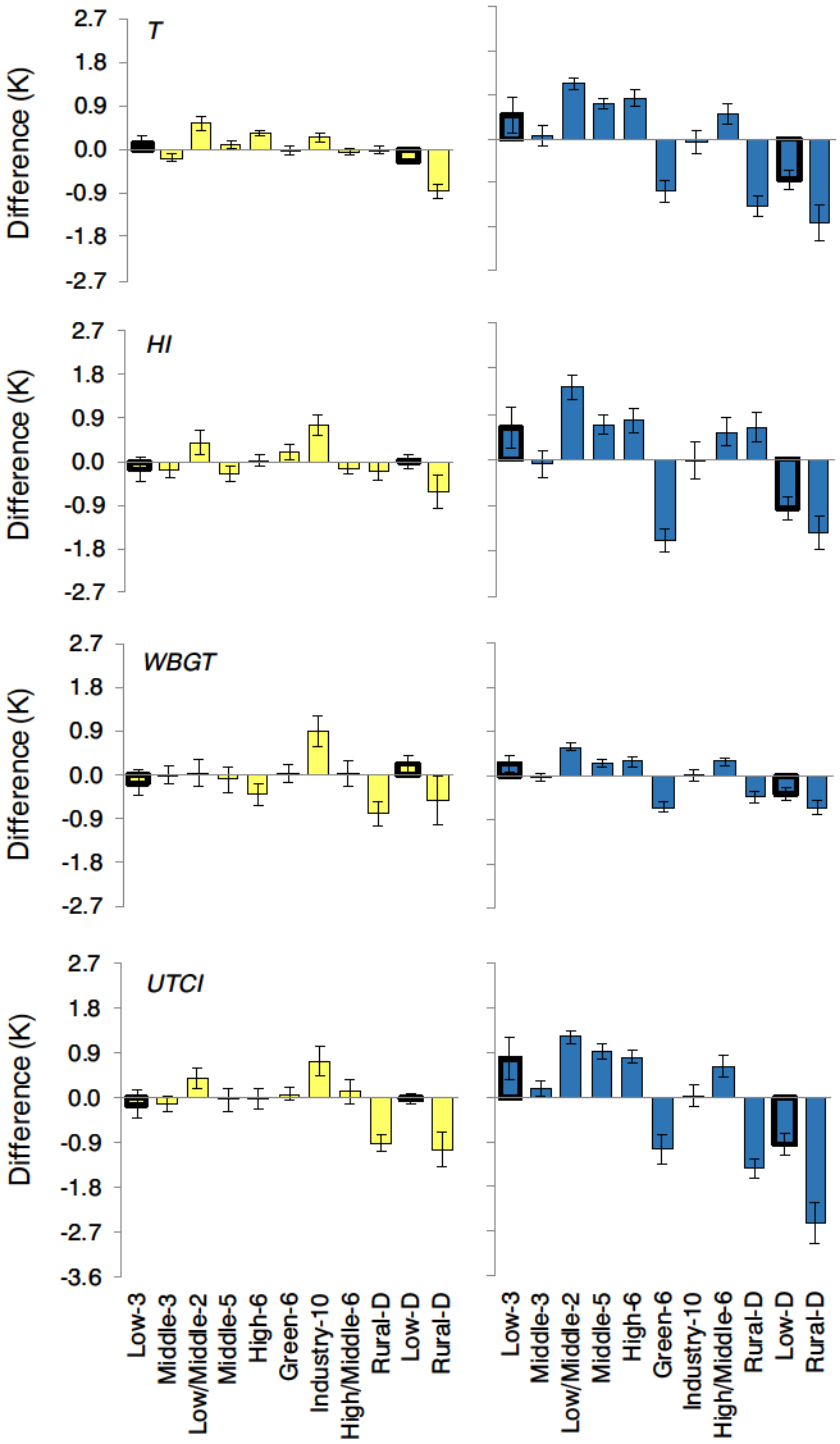

Fig. 7. As in Fig. 5, but for Faisalabad.

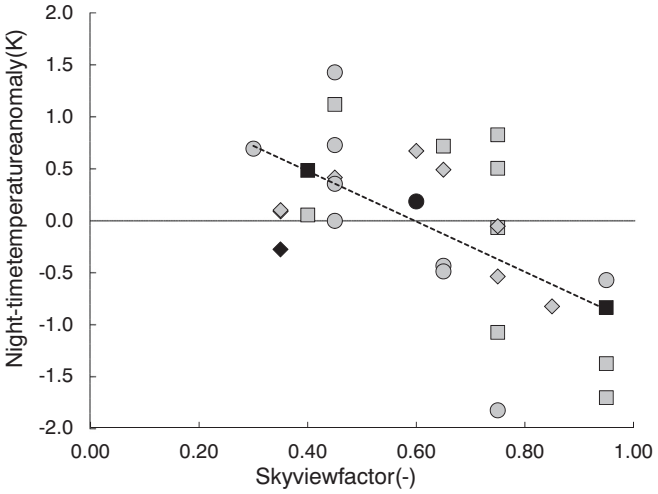

Fig. 8. Observed average night-time air temperature anomaly versus sky view factor from LCZ classification (middle value per class, see Table 1), for Delhi (circles), Dhaka (diamonds) and Faisalabad (squares). Bold symbols denote low-income neighbourhoods. The regression line is described by y = 1.45 2.43x (r^2 = 0.38).

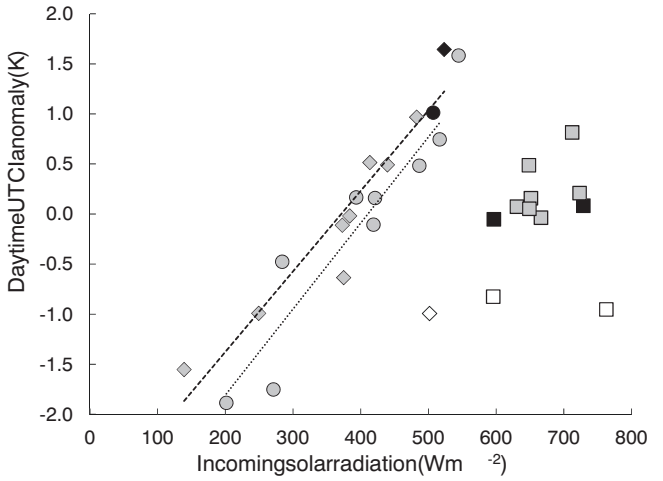

Fig. 9. Average UTCI anomaly versus average incoming solar radiation for Delhi (circles), Dhaka (diamonds) and Faisalabad (squares). Bold data points indicate low-income neighbourhoods, open data points "Rural" areas. The regression line for Delhi (dots) is described by y = 0.0091x 3.7 (r^2 = 0.90) and the one for Dhaka (dashes), excluding the rural observation, by y = 0.0080x 3.0 (r^2 = 0.91).

relationship between night-time temperature anomalies and sky view factor. However, it also shows that the low-income neighbourhoods may or may not be warmer. Three out of the four low-income neighbourhoods belong to the warmer ones during the night, one is comparatively cool.

Transects that are found to be cool during the night may become comparatively warm or around average during the day, for example, "Low-Middle 6" in Dhaka and "Green-6" in Faisalabad. These effects can be explained by shading effects at street level. Especially during dry periods, lack of shading in open areas may lead to stronger warming and vice versa (Giridharan and Emmanuel, 2018).

We now turn to differences according to the thermal comfort indices. For the night-time runs, the general pattern of the differences between neighbourhoods along the transect was found to be approximately similar in terms of the thermal comfort indices and temperature. That is, the spatial differences according to the heat indices are highly correlated with the air temperature differences. However, during the day marked differences occurred between the indices or variables that consider radiation, WBGT and UTCI, and the ones that do not, *T* and HI. The radiation-driven indices underline that open neighbourhoods may become comparatively warm under the influence of the solar radiation, whereas the densely built neighbourhoods (LCZ 1–3, 7) can in fact become cooler because of shading effects. However, again the patterns are not entirely consistent with this principle. Both in Delhi and in Dhaka some of the dense neighbourhoods are among the warmest in terms of UTCI, WBGT or both. Among the notable exceptions are the low-income neighbourhoods Low-2 in Delhi and Low-7 in Dhaka. This is partly related to the higher air temperatures in those neighbourhoods, but exposure to radiation plays an important role. Like will be shown below the dense building style does not automatically provide protection against the sun.

Differences in the radiation environment along the transect also explain that for WBGT and UTCI the range of x′ (see Eq. (4)) is larger during daytime than during night-time for Delhi and Dhaka. However, for Faisalabad the daytime differences are smaller. Here, differences in WBGT and UTCI are mainly caused by temperature because the radiation conditions along the transect are relatively uniform. This city mainly consists of low-rise buildings (LCZ classes 3 and 6, see Fig. 2 and Table 1).

This is further illustrated in Fig. 9, which depicts the seasonal averages of the daytime spatial anomalies of UTCI versus incoming solar radiation in the neighbourhoods. The average radiation intensities span a much larger range in Delhi and Dhaka (343 and 384Wm ^{2}, respectively) than in Faisalabad (167Wm ^{2}). Thus, daytime UTCI anomaly ranges are also larger in Delhi and Dhaka (3.47 and 3.23 K, respectively) than in Faisalabad (1.77 K). Three anomalies for neighbourhoods classified as "Rural" (recognizable as open symbols in the graph) clearly stand out and may show that green areas can bring some relief of heat, even if radiation levels are high. In Delhi and Dhaka, the patterns of measured average radiation intensity in built neighbourhoods explain just over 90% of the UTCI anomalies. Similar relationships are found for WBGT (not shown here), with radiation intensity explaining about 81% and 91% of the mean WBGT anomalies in Delhi and Dhaka, respectively. In Delhi and Dhaka, high radiation intensities have been measured in the low-income neighbourhoods, despite the high building density (bold symbols in the figure). The results in Faisalabad show that during daytime the low-income neighbourhoods may be among the cooler ones in terms of UTCI. Shading as well as relatively green surroundings like in Faisalabad may reduce heat in any neighbourhood. As such, the results underline the importance of opportunities to access shaded areas that provide relief from heat during hot periods as well as important influences of the surroundings of such neighbourhoods.

Humidity may play a significant role too, which is best illustrated by means of HI. According to that index, the greener open areas may also be perceived as slightly warmer during daytime (Figs. 5–7). For example, "High 6" and "Middle 5" in Delhi are more open and greener neighbourhoods, which are cooler on average in terms of daytime T, but show a higher HI. Since this index only responds to air temperature and humidity the higher value of HI must be due to a higher average humidity.

Intra-urban spatial differences and differences between low- and high-income neighbourhoods were further investigated for night-time conditions. Fig. 10 shows the maximum air temperature differences along the transects observed during the individual traverses and during the season. Hardly any seasonal trend was found in the maximum intra-urban temperature difference. This was also true for the heat indices (not shown here). A weak tendency was found for Delhi and for Faisalabad. Here maximum air temperature differences tended to decrease after the onset of the monsoon, whereas such tendencies were virtually absent in Dhaka.

In Fig. 10, the mean temperature differences between the low- and high-income neighbourhoods are indicated with pluses if the low-income ones are warmer and with minuses if they are cooler. The low-income neighbourhood in Delhi is always warmer during the

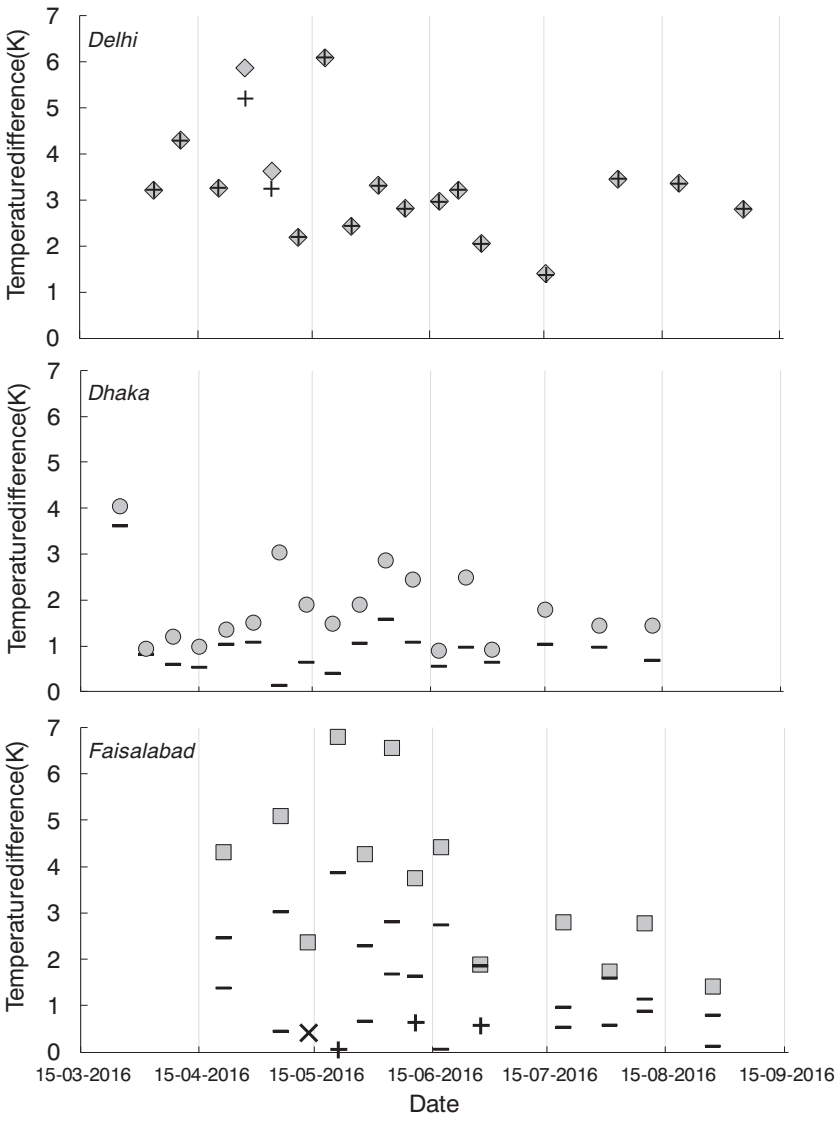

Fig. 10. Observed maximum intra-urban night-time temperature differences along the transects in Delhi (upper, diamonds), Dhaka (middle, circles) and Faisalabad (lower, squares) and comparison with the temperature differences between low-income and high-income neighbourhoods (Low-2 – High-6 in Delhi; Low-7 – High-2 in Dhaka; Low-3 – High-6 and Low-D – High-6 in Faisalabad, respectively; see Table 1). Plus: low-income neighbourhood is warmer; minus: low-income neighbourhood is cooler. X: one negative and one positive difference of nearly equal absolute value.

night and the differences nearly always represent the maximum intra-urban difference. However, in Dhaka and Faisalabad the low-income neighbourhoods are always (Dhaka) or usually (Faisalabad) cooler, but the differences hardly ever represent the maximum intra-urban difference. This is consistent with the observation that both the low-income neighbourhood and the high-income neighbourhood may be systematically warmer or cooler than the average (see Figs. 5–7).

4. Discussion and conclusions

In this paper we assess temporal and spatial patterns of exposure to heat in three major cities in South Asia: Delhi (India), Dhaka (Bangladesh) and Faisalabad (Pakistan). Our results show extremely high temperatures and heat index values over prolonged periods of time in these cities. Maximum daytime values of HI, WBGT and UTCI indicate potentially dangerously hot conditions on many days in the boreal summer season, ranging from nearly 50% of the days according to HI in Delhi, and up to 100% of the days according to WBGT in Dhaka in the period investigated here (Table 2). This supports the hypothesis that people in low-income countries may be living in so-called climatic hot spots (De Souza et al., 2015) with enhanced exposure to climate threats including heat. Yet, the observations presented in this paper nuance the idea that people living in informal neighbourhoods are consistently more exposed to heat than people in richer neighbourhoods.

During night-time, compact neighbourhoods tend to remain warmer than more open neighbourhoods (Fig. 8), in accordance with UHI theory. Of the neighbourhoods included in the present study, a majority (8 out of 11) of the low- to low- and middle-income neighbourhoods belong to such compact classes, LCZ 1–3 and LCZ 7 (see Table 1 and Figs. 5–7). However, some of the richer neighbourhoods also belong to compact classes, whereas some of the lower-income neighbourhoods are built in a less compact style.

The results are consistent with the idea laid down in the LCZ concept that densely built neighbourhoods are expected to cool down more slowly than open, sparsely built neighbourhoods (Stewart and Oke, 2012). Yet, the interpretation is not straightforward. Actual day-to-day patterns may depend on the weather (He, 2018), the season and the actual building height and width of streets. Whereas the lower sky view of

the dense neighbourhoods hampers nocturnal radiative cooling, abundance of shading during daytime may lead to less storage of heat, depending on the aforementioned characteristics (Theeuwes et al., 2014) and other neighbourhood characteristics like the amount of green and the presence of water bodies (Gunawardena et al., 2017).

An important consideration is the fact that people spend a significant fraction of their time indoors, especially during night-time. Enhanced exposure during night-time to indoor conditions is particularly relevant, because of possible health effects due to reduced quality of sleep (Obradovich et al., 2017). In the present context it is therefore interesting to explore the possible impact of differences in outdoor thermal conditions on indoor temperatures (Franck et al., 2013; Liao et al., 2015; Nguyen et al., 2014). In particular for naturally ventilated houses without air conditioning and with uninsulated tin roofs, tin walls, or both, present in the informal neighbourhoods in Delhi and Dhaka, a reasonably strong relationship between indoor and outdoor temperature may be expected. For such houses, neighbourhood differences in the outdoor temperature will result in indoor temperature differences as well. This could imply that indoor temperatures are higher in informal neighbourhoods in cases where their outdoor environment is warmer. This would be interesting to study further.

During the night, average outdoor heat patterns revealed by the more complicated UTCI and WBGT are reasonably consistent with the ones from air temperature and HI, obviously because solar radiation and shading play no direct role during night-time. This indicates that night-time patterns of heat can be described by relatively simple indices. During daytime, however, solar radiation and wind patterns are crucial. Larger fractions of the densely built neighbourhoods may provide shading at street level, thereby locally improving human thermal comfort in comparison with more open neighbourhoods (Emmanuel et al., 2007). This important role of solar radiation is described best by means of indicators like UTCI and WBGT. Their spatial patterns are quite different from the ones of T and HI. The data also show that in low-income neighbourhoods, protection against heat by shading is not guaranteed. Actual exposure to sun will depend on factors such as orientation of streets in combination with solar angle, placement of objects providing shade, among other things (Oke et al., 2017). Obviously shaded spots can also be found in more open neighbourhoods, independent of socio-economic status. In addition to such local shading effect, if dense neighbourhoods are embedded in, or surrounded by, green/blue open areas they may offer a bit of cooling rather than being just hot spots, such as, for example, in Dhaka for “Low 7” or in Faisalabad for “Low 2”.

Our analyses underline that it is important to consider heat indices that account for radiation when considering heat exposure of humans, especially during daytime when solar radiation is crucial. Seasonal trends differ among the various indicators (Fig. 4.). This is an important consideration when designing heat-health action plans. Whereas it has since long been known that for assessment of the thermal influence of the environment of heat all parameters relevant for the human energy balance should be accounted for (Höppe, 1999), such plans are often still based only on forecasts of temperature (World Health Organization, 2018; Knowlton et al., 2014). In particular when calibrated on mortality statistics, the skill of simple indices to forecast dangerous days with an increased number of fatalities has been found to be quite reasonable (Hajat et al., 2010b). However, such forecasts are typically based on extra-urban conditions. It is important to recognize that urban growth will continue (United Nations, 2014) and an increasing number of people will be exposed to heat in urban environments. Recent urban climate research has shown that detailed forecasts of heat in cities are within reach (Ronda et al., 2017) and even reliable forecasts of advanced thermal comfort indices like UTCI and WBGT within urban environments can be made (Leroyer et al., 2018). The results from the present study support the idea of developing heat action plans based on such forecasts, especially in urban environments. It is recommended to further explore possibilities of using radiation-driven indices within urban environments as triggers for heat action plans. Results shown in Fig. 4 show that it is likely that this would also improve heat-event forecasts outside typical heatwave periods.

Our findings provide context to policy challenges of adapting to current climate extreme and future climate change. The observed intra-urban temperature differences, though relatively modest, suggest that climate smart city design can help alleviating the burden of a rise in temperature due to climate change. To put this into perspective: limiting global temperature rise to 1.5 K, instead of 2 K - a difference of just 0.5 K -, could decrease extreme heat-related mortality by 15–22% per summer in European cities (Mitchell et al., 2018). Neighbourhoods, and not only the rich ones, should be designed such that they provide shading during the day, but also be intersected or embedded in open green spaces to provide cooling during the night. Cities in South Asia and other developing countries face numerous other pressing development challenges, from improving transport and improving air quality to improving housing. Yet, this development provides a window of opportunity; much of South Asia's infrastructure of the future still needs to be built. There is a choice to build it climate smart.

Supplementary data to this article can be found online at https://doi.org/10.1016/j.scitotenv.2019.04.087.

Acknowledgements

This work was carried out by the Himalayan Adaptation, Water and Resilience (HI-AWARE) consortium under the Collaborative Adaptation Research Initiative in Africa and Asia (CARIAA) with financial support from the UK Government's Department for International Development (DFID), London, UK, and the International Development Research Centre (IDRC), Ottawa, Canada. We are indebted to Jan Elbers, our technical assistant and colleague before he decided to put his many talents in the service of *Doctors without Borders*. Jan designed the mobile devices, set-up the AWS, and did a first screening and processing of the measurements. We would like to thank Richa Sharma of the National Institute of Urban Affairs in New Delhi for providing us with an initial LCZ map of Delhi based on the UrbClim project work, which helped us designing an improved LCZ classification for our neighbourhoods and Delhi as a whole. Mr. Sushanto Gupta of BCAS helped with creating the LCZ map of Dhaka. Muhammad Adrees, Kousik Ahmed, Sana Ehsan, Simson Halder, Fatima Noor, Prasoon Singh, Kaagita Venkatramana and Daniël Zweeckhorst helped with conducting the measurements. We thank the two anonymous reviewers for their valuable comments that helped to improve the manuscript.

Disclaimer

The views expressed in this work are those of the creators and do not necessarily represent those of the UK Government's Department for International Development, the International Development Research Centre, Canada, or its Board of Governors.

References

Abbas, F., 2013. Analysis of a historical (1981–2010) temperature record of the Punjab province of Pakistan. Earth Interact., 17-015 https://doi.org/10.1175/2013EI000528.1.

Armson, D., Stringer, P., Ennos, A.R., 2012. The effect of tree shade and grass on surface and globe temperatures in an urban area. Urban For. Urban Green. 11, 245–255.

Azhar, G.S., Mavalankar, D., Nori-Sarma, A., Rajiva, A., Dutta, P., Jaiswal, A., et al., 2014. Heat-related mortality in India: excess all-cause mortality associated with the 2010 Ahmedabad heat wave. PLoS One 9, e91831. https://doi.org/10.1371/journal.pone.0091831.

Bangladesh Bureau of Statistics, 2014. Bangladesh Population and Housing Census 2011, Urban Area Report, Statistics and Informatics Division, Ministry of Planning, Government of Bangladesh. vol. 3. Government of the people's republic of Bangladesh. www.bbs.gov.bd.

Bathiany, S., Dakos, V., Scheffer, M., Lenton, T.M., 2018. Climate models predict increasing temperature variability in poor countries. Sci. Adv. 4.

Bechtel, B., Alexander, P., Böhner, J., Ching, J., Conrad, O., Feddema, J., et al., 2015. Mapping local climate zones for a worldwide database of the form and function of cities. ISPRS International Journal of Geo-Information 4, 199.

Blazejczyk, K., Epstein, Y., Jendritzky, G., Staiger, H., Tinz, B., 2012. Comparison of UTCI to selected thermal indices. Int. J. Biometeorol. 56, 515–535.
Brode, P., Fiala, D., Blazejczyk, K., Holmer, I., Jendritzky, G., Kampmann, B., et al., 2012. Deriving the operational procedure for the Universal Thermal Climate Index (UTCI). Int. J. Biometeorol. 56, 481–494.
Budd, G.M., 2015. Wet-bulb globe temperature (WBGT) - its history and its limitations. J. Sci. Med. Sport 11, 20–32.
Collins, M., Knutti, R., Arblaster, J., Dufresne, J.-L., Fichefet, T., Friedlingstein, P., et al., 2013. Long-term climate change: projections, commitments and irreversibility. In: Stocker, T.F., Qin, D., Plattner, G.-K., Tignor, M., Allen, S.K., Boschung, J., et al. (Eds.), Climate Change 2013: The Physical Science Basis. Contribution of Working Group I to the Fifth Assessment Report of the Intergovernmental Panel on Climate Change. Cambridge University Press Cambridge, United Kingdom and New York, NY, USA.
de Freitas, C.R., Grigorieva, E.A., 2017. A comparison and appraisal of a comprehensive range of human thermal climate indices. Int. J. Biometeorol. 61, 487–512.
De Souza, K., Kituyi, E., Harvey, B., Leone, M., Murali, K.S., Ford, J.D., 2015. Vulnerability to climate change in three hot spots in Africa and Asia: key issues for policy-relevant adaptation and resilience-building research. Reg. Environ. Chang. 15, 747–753.
Emmanuel, R., Rosenlund, H., Johansson, 2007. Urban shading—a design option for the tropics? A study in Colombo, Sri Lanka. Int. J. Climatol. 27, 1995–2004.
Fiala, D., Havenith, G., Brode, P., Kampmann, B., Jendritzky, G., 2012. UTCI-Fiala multi-node model of human heat transfer and temperature regulation. Int. J. Biometeorol. 56, 429–441.
Field, A.P., Miles, J., Field, Z., 2012. Discovering statistics using R. http://dspace.fue.edu.eg/xmlui/handle/123456789/2902.
Franck, U., Krüger, M., Schwarz, N., Grossmann, K., Röder, S., Schlink, U., 2013. Heat stress in urban areas: indoor and outdoor temperatures in different urban structure types and subjectively reported well-being during a heat wave in the city of Leipzig. Meteorol. Z. 22, 167–177.
Giridharan, R., Emmanuel, R., 2018. The impact of urban compactness, comfort strategies and energy consumption on tropical urban heat island intensity: a review. Sustain. Cities Soc. 40, 677–687.
Gunawardena, K.R., Wells, M.J., Kershaw, T., 2017. Utilising green and bluespace to mitigate urban heat island intensity. Sci. Total Environ. 584–585, 1040–1055.
Hajat, S., O'Connor, M., Kosatsky, T., 2010a. Health effects of hot weather: from awareness of risk factors to effective health protection. Lancet 375, 856–863.
Hajat, S., Sheridan, S.C., Allen, M.J., Pascal, M., Laaidi, K., Yagouti, A., et al., 2010b. Heat–health warning systems: a comparison of the predictive capacity of different approaches to identifying dangerously hot days. Am. J. Public Health 100, 1137–1144.
Havenith, G., Fiala, D., Blazejczyk, K., Richards, M., Brode, P., Holmer, I., et al., 2012. The UTCI-clothing model. Int. J. Biometeorol. 56, 461–470.
He, B.-J., 2018. Potentials of meteorological characteristics and synoptic conditions to mitigate urban heat island effects. Urban Climate 24, 26–33.
Heusinkveld, B.G., Steeneveld, G.J., van Hove, L.W.A., Jacobs, C.M.J., Holtslag, A.A.M., 2014. Spatial variability of the Rotterdam urban heat island as influenced by urban land use. J. Geophys. Res.-Atmos. 119, 677–692.
Hondula, D.M., Balling, R.C., Andrade, R., Scott Krayenhoff, E., Middel, A., Urban, A., et al., 2017. Biometeorology for cities. Int. J. Biometeorol. 61, 59–69.
Höppe, P., 1999. The physiological equivalent temperature—a universal index for the biometeorological assessment of the thermal environment. Int. J. Biometeorol. 43, 71–75.
India Census, 2015. Delhi population 2011–2018 census. https://www.census2011.co.in/census/state/delhi.html.
Jendritzky, G., de Dear, R., Havenith, G., 2012. UTCI—why another thermal index? Int. J. Biometeorol. 56, 421–428.
Klemm, W., Heusinkveld, B.G., Lenzholzer, S., van Hove, B., 2015. Street greenery and its physical and psychological impact on thermal comfort. Landsc. Urban Plan. 138, 87–98.
Knowlton, K., Kulkarni, S., Azhar, G., Mavalankar, D., Jaiswal, A., Connolly, M., et al., 2014. Development and implementation of South Asia's first heat-health action plan in Ahmedabad (Gujarat, India). Int. J. Environ. Res. Public Health 11, 3473.
Kotharkar, R., Ramesh, A., Bagade, A., 2018. Urban heat island studies in South Asia: a critical review. Urban Climate 24, 1011–1026.
Leichenko, R., Silva, J.A., 2014. Climate change and poverty: vulnerability, impacts, and alleviation strategies. Wiley Interdiscip. Rev. Clim. Chang. 5, 539–556.
Leroyer, S., Bélair, S., Spacek, L., Gultepe, I., 2018. Modelling of radiation-based thermal stress indicators for urban numerical weather prediction. Urban Climate 25, 64–81.
Liao, F.-C., Cheng, M.-J., Hwang, R.-L., 2015. Influence of urban microclimate on air-conditioning energy needs and indoor thermal comfort in houses. Adv. Meteorol. 2015.
Liljegren, J.C., Carhart, R.A., Lawday, P., Tschopp, S., Sharp, R., 2008. Modeling the wet bulb globe temperature using standard meteorological measurements. J. Occup. Environ. Hyg. 5, 645–655.
Minallah, M., Ghaffar, A., Shirazi, S.A., 2012. Remote sensing and GIS applications for monitoring and assessment of the urban sprawl in Faisalabad-Pakistan. Pak. J. Sci. 64, 203–208.
Mitchell, D., Heaviside, C., Schaller, N., Allen, M., Ebi, K.L., Fischer, E.M., Gasparrini, A., Harrington, L., Kharin, V., Shiogama, H., Sillmann, J., Sippel, S., Vardoulakis, S., 2018. Extreme heat-related mortality avoided under Paris Agreement goals. Nat. Clim. Chang. 8, 551–553.
Mohan, M., Kikegawa, Y., Gurjar, B.R., Bhati, S., Kandya, A., Ogawa, K., 2012. Urban heat island assessment for a tropical urban airshed in India. Atmospheric and Climate Sciences 02 (02), 12.
Mohan, M., Kikegawa, Y., Gurjar, B.R., Bhati, S., Kolli, N.R., 2013. Assessment of urban heat island effect for different land use-land cover from micrometeorological measurements and remote sensing data for megacity Delhi. Theor. Appl. Climatol. 112, 647–658.
Mora, C., Dousset, B., Caldwell, I.R., Powell, F.E., Geronimo, R.C., Bielecki Coral, R., et al., 2017. Global risk of deadly heat. Nat. Clim. Chang. 7, 501–506.
Nguyen, J.L., Schwartz, J., Dockery, D.W., 2014. The relationship between indoor and outdoor temperature, apparent temperature, relative humidity, and absolute humidity. Indoor Air 24, 103–112.
Nikolopoulou, M., Steemers, K., 2003. Thermal comfort and psychological adaptation as a guide for designing urban spaces. Energ. Buildings 35, 95–101.
Obradovich, N., Migliorini, R., Mednick, S.C., Fowler, J.H., 2017. Nighttime temperature and human sleep loss in a changing climate. Sci. Adv. 3, e1601555.
Oke, T.R., 1982. The energetic basis of the urban heat-island. Q. J. R. Meteorol. Soc. 108, 1–24.
Oke, T.R., Mills, G., Christen, A., Voogt, J.A., 2017. Urban Climates. Urban Climates. Cambridge University Press, Cambridge (525 pp.).
Ooi, G.L., Phua, K.H., 2007. Urbanization and slum formation. J. Urban Health 84, 27–34.
Pakistan Bureau of Statistics, 2018. http://www.pbscensus.gov.pk/, Accessed date: 18 April 2018.
R Core Team, 2013. R: a language and environment for statistical computing. R foundation for Statistical Computing, Vienna, Austria URL. http://www.R-project.org/.
Revi, A., Satterthwaite, D.E., Aragón-Durand, F., Corfee-Morlot, J., Kiunsi, R.B., Pelling, M., et al., 2014. Urban areas. In: Field, C.B., Barros, V.R., Dokken, D.J., Mach, K.J., Mastrandrea, M.D., Bilir, T.E., et al. (Eds.), Climate Change 2014: Impacts, Adaptation, and Vulnerability. Part A: Global and Sectoral Aspects. Contribution of Working Group II to the Fifth Assessment Report of the Intergovernmental Panel on Climate Change, pp. 535–612.
Ronda, R.J., Steeneveld, G.J., Heusinkveld, B.G., Attema, J.J., Holtslag, A.A.M., 2017. Urban finescale forecasting reveals weather conditions with unprecedented detail. Bull. Am. Meteorol. Soc. 98, 2675–2688.
Saeed, F., Salik, K.M., Ishfaq, S., 2016. Climate Induced Rural-to-Urban Migration in Pakistan: PRISE Working Paper. Available online at:. http://prise.odi.org/wp-content/uploads/2016/01/Low_Res-Climate-induced-rural-to-urban-migration-in-Pakistan.pdf.
Santamouris, M., 2015. Analyzing the heat island magnitude and characteristics in one hundred Asian and Australian cities and regions. Sci. Total Environ. 512, 582–598.
Sati, A.P., Mohan, M., 2017. The impact of urbanization during half a century on surface meteorology based on WRF model simulations over National Capital Region, India. Theor. Appl. Climatol. 1–15.
Shastri, H., Barik, B., Ghosh, S., Venkataraman, C., Sadavarte, P., 2017. Flip flop of day-night and summer-winter surface urban heat island intensity in India. Sci. Rep. 7, 8.
Sherwood, S.C., Huber, M., 2010. An adaptability limit to climate change due to heat stress. Proc. Natl. Acad. Sci. 107, 9552–9555.
Singh, T., Siderius, C., Van der Velde, Y., 2018. When do Indians feel hot? Internet searches indicate seasonality suppresses adaptation to heat. Environ. Res. Lett. 13, 054009.
Smith, S.R., Bourassa, M.A., 1996. http://coaps.fsu.edu/woce/truewind/f-codes/truewind.f, Accessed date: 15 March 2019.
Steadman, R.G., 1979a. The assessment of sultriness. Part I: a temperature-humidity index based on human physiology and clothing science. J. Appl. Meteorol. 18, 861–873.
Steadman, R.G., 1979b. The assessment of sultriness. Part II: effects of wind, extra radiation and barometric pressure on apparent temperature. J. Appl. Meteorol. 18, 874–885.
Stewart, I.D., Oke, T.R., 2012. Local climate zones for Urban temperature studies. Bull. Am. Meteorol. Soc. 93, 1879–1900.
Sverdlik, A., 2011. Ill-health and poverty: a literature review on health in informal settlements. Environ. Urban. 23, 123–155.
Theeuwes, N.E., Steeneveld, G.J., Ronda, R.J., Heusinkveld, B.G., van Hove, L.W.A., Holtslag, A.A.M., 2014. Seasonal dependence of the urban heat island on the street canyon aspect ratio. Q. J. R. Meteorol. Soc. 140, 2197–2210.
Theeuwes, N.E., Steeneveld, G.-J., Ronda, R.J., Holtslag, A.A.M., 2017. A diagnostic equation for the daily maximum urban heat island effect for cities in northwestern Europe. Int. J. Climatol. 37, 443–454.
Thorsson, S., Lindberg, F., Eliasson, I., Holmer, B., 2007. Different methods for estimating the mean radiant temperature in an outdoor urban setting. Int. J. Climatol. 27, 1983–1993.
Tzavali, A., Paravantis, J.P., Mihalakakou, G., Fotiadi, A., Stigka, E., 2015. Urban heat island intensity: a literature review. Fresenius Environ. Bull. 24, 4535–4554.
United Nations, Department of Economic and Social Affairs, Population Division, 2014. World Urbanization Prospects: The 2014 Revision (CD-ROM Edition).
Van Hove, L.W.A., Jacobs, C.M.J., Heusinkveld, B.G., Elbers, J.A., van Driel, B.L., Holtslag, A.A.M., 2015. Temporal and spatial variability of urban heat island and thermal comfort within the Rotterdam agglomeration. Build. Environ. 83, 91–103.
Weatherbase, 2018a. . Delhi, India. http://www.weatherbase.com/weather/weather.php3?s=28124, Accessed date: 15 November 2018.
Weatherbase, 2018b. . Dhaka, Bangladesh. http://www.weatherbase.com/weather/weather.php3?s=32914, Accessed date: 15 November 2018.
Weatherbase, 2018c. . Faisalabad, Pakistan. http://www.weatherbase.com/weather/weather.php3?s=592583, Accessed date: 15 November 2018.
World Health Organization (WHO), 2018. Heat-health action plans, guidance. WHO Regional Office for Europe http://www.euro.who.int/__data/assets/pdf_file/0006/95919/E91347.pdf.
Yadav, N., Sharma, C., 2018. Spatial variations of intra-city urban heat island in megacity Delhi. Sustain. Cities Soc. 37, 298–306.